Mono Axial Vehicle platform for education purposes

Jozef Rodina
Institute of Control and Industrial Informatics
FEI STU
Bratislava, Slovak Republic
jozef.rodina@stuba.sk

Peter Hubinsky
Institute of Control and Industrial Informatics
FEI STU
Bratislava, Slovak Republic
peter.hubinsky@stuba.sk

***Abstract*—This paper presents a concept of the Mono Axial Vehicle (MAV) platform for education purposes. The chassis of the MAV can rotate around the wheel axis, hence the system behavior is changing with rotation of the chassis. This allows development of the different control methods on the same vehicle platform. Chassis of the MAV is made of composite materials and the wheels are made of aluminum. The control board is based on 16-bit DSP microcontroller and MEMS sensors. It is able to control up to six servos. Additional sensors may also be added. In order to speed up development, the C libraries and MATLAB based dynamic model are available.**

Keywords-mono axial vehicle, inverted pendulum, oscillation damping, ZVD shaper, LQ regulator, DSP, MEMS

I. INTRODUCTION

Mono axial vehicle (Fig.1) is a very interesting platform for design and evaluation of control methods for movement systems [1]. A system behaviour can be described like an inverted pendulum (centre of gravity of the chassis is located above the wheels axis) and a classical pendulum/two-mass system (centre of gravity of the chassis is located under the wheels axis). Therefore different control methods have to be used.

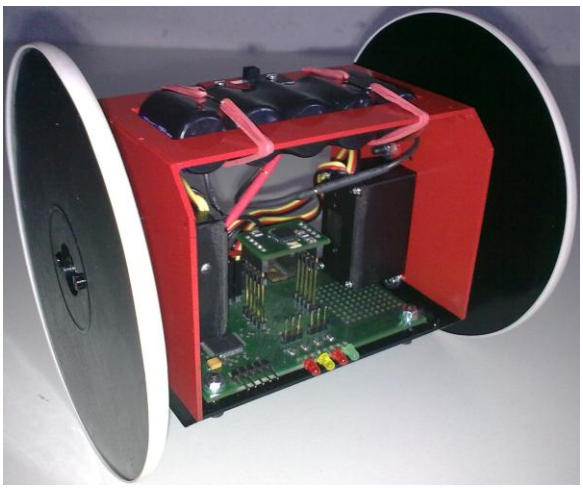

Figure 1. Mono Axial vehicle

The system in upper position is unstable therefore we have to use stabilization control. The LQR controller is used for this case. The system has tendency to oscillate in lower position. We are using two methods for oscillation damping: input signal shaper (feed-forward methods) and derivative feedback. A block diagram of the motion control is shown in Fig.2. All these control methods have been tested in MATLAB SIMULINK.

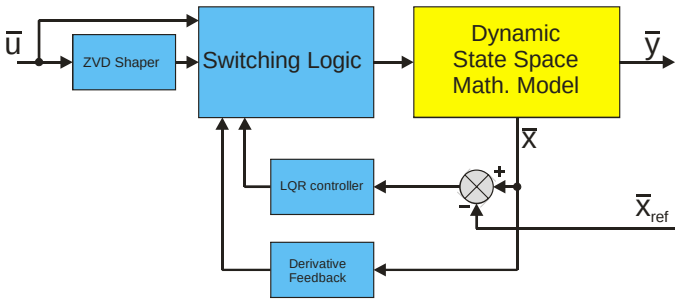

Figure 2. Principal scheme of the motion control of the Mono axial vehicle

II. MATHEMATICAL MODEL

The MAV used two motors for its motion and this cause that not only straightforward motion is possible, but we consider only straightforward motion in mathematical model. In order to develop the control system, we need to create a mathematical model of system that will be corresponding with behaviour of the real system. This system behaviour is similar to pendulum on wheels. The body, wheel and DC motor dynamic are analyzed separately at the beginning, but in the end we will get two nonlinear equations of motion that completely describes dynamic of the vehicle. These equations are nonlinear, but in our case of the hybrid control system we have to linearise them.

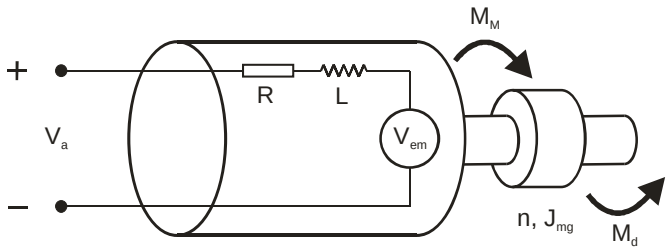

Figure 3. Diagram of DC motor

According to the Fig. 3 the following equations for DC motor can be defined:

$$M_M = Cu.i.n \tag{1}$$

$$\dot{\omega} = \frac{Cu.n}{J_{mg}.R} V_a - \frac{Cu^2.n}{J_{mg}.R}\omega - \frac{M_d}{J_{mg}} \tag{2}$$

where:

M_M	torque produced by DC motor
Cu	torque constant
i	current generated in the motor armature
n	gearbox moment gain
ω	output shaft angular velocity
$\dot{\omega}$	output shaft angular acceleration
J_{mg}	moment of inertia of the motor and gearbox
M_d	disturbance torque on output shaft
R	rotor winding resistance
V_a	voltage applied on a motor terminals

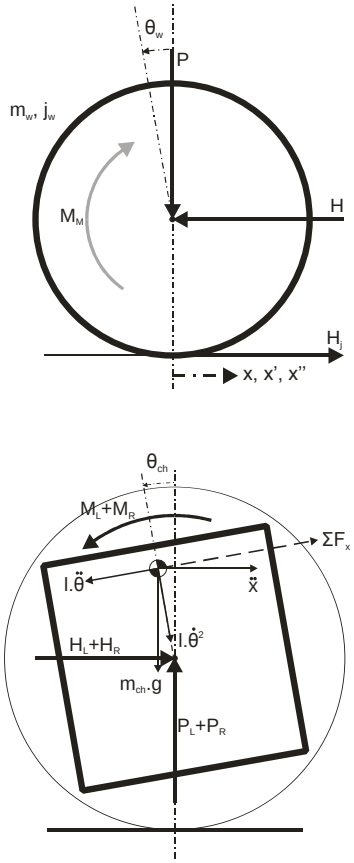

Figure 4. Free body diagram of the wheel and the chassis

For the wheel and the chassis (Fig.4)

$$(m_w + \frac{J_w}{r^2})\ddot{x} = \frac{Cu.n}{R.r}V_a - \frac{Cu^2.n}{R.r^2}\dot{x} - H \tag{3}$$

$$H_L + H_R = m_{ch}.l.\ddot{\theta}\cos\theta - m_{ch}.l.\dot{\theta}^2 + m_{ch}.\ddot{x} \tag{4}$$

$$(H_L + H_R).l.\cos\theta + (P_L + P_R).l.\sin\theta - m_{ch}.g.\sin\theta - m_{ch}.l.\ddot{\theta} = m_{ch}.\ddot{x}.\cos\theta \tag{5}$$

$$-(H_L + H_R).l.\cos\theta - (P_L + P_R).l.\sin\theta - (M_L + M_R) = J_{ch}\ddot{\theta} \tag{6}$$

where:

m_w	wheel mass
r	wheel radius
J_w	moment of inertia of the wheel
$\dot{x}, \ddot{x}$	wheel velocity, wheel acceleration
m_{ch}	chassis mass
l	distance from center of the chassis to the center of gravity of the chassis
J_{ch}	moment of inertia of the chassis
H	force
P	force
$\theta_{ch}, \dot{\theta}_{ch}, \ddot{\theta}_{ch}$	angle, angular velocity and angular acceleration of chassis
$\theta_w, \dot{\theta}_w, \ddot{\theta}_w$	angle, angular velocity and angular acceleration of wheel

By rearranging and combining equations 1 - 6 we get the non-linear equations of motion of the mono axial vehicle:

$$\ddot{\theta}(J_{ch} + m_{ch}l^2) = \frac{2Cu^2n}{Rr}\dot{x} - m_{ch}.l.\cos\theta\,\ddot{x} - m_{ch}.l.g.\sin\theta - \frac{Cu.n}{Rr}(V_{AL} + V_{AR}) \tag{7}$$

$$\ddot{x}(2m_{ch}+\frac{2J_w}{r^2}+m_{ch})=\frac{2Cu^2n}{Rr^2}\dot{x}-m_{ch}.l.\cos\theta\ddot{\theta}- \quad (8)$$
$$-m_{ch}.l.\sin\theta\ddot{\theta}^2+\frac{Cu.n}{Rr}(V_{AL}+V_{AR})$$

These two equations above can be linearised in a surround of upward position. Therefore:

$$\cos\theta=-1 \qquad \sin\theta=-\theta \qquad \frac{d\theta}{dt}=0$$

We get:

$$\ddot{\theta}(J_{ch}+m_{ch}l^2)=m_{ch}.l.\ddot{x}+\frac{2Cu^2n}{Rr}\dot{x}+ \quad (9)$$
$$+m_{ch}.l.g.\theta-\frac{Cu.n}{Rr}(V_{AL}+V_{AR})$$

$$\ddot{x}(2m_{ch}+\frac{2J_w}{r^2}+m_{ch})=\frac{2Cu^2n}{Rr^2}\dot{x}+m_{ch}.l.\ddot{\theta}+ \quad (10)$$
$$+\frac{Cu.n}{Rr}(V_{AL}+V_{AR})$$

$$\ddot{\theta}=\frac{m_{ch}.l}{(J_{ch}+m_{ch}l^2)}.\ddot{x}+\frac{2Cu^2n}{(J_{ch}+m_{ch}l^2)Rr}\dot{x}+ \quad (11)$$
$$+\frac{m_{ch}.l.g.\theta}{(J_{ch}+m_{ch}l^2)}-\frac{Cu.n}{(J_{ch}+m_{ch}l^2)Rr}(V_{AL}+V_{AR})$$

$$\ddot{x}=\frac{2Cu^2n}{(2m_{ch}+\frac{2J_w}{r^2}+m_{ch})Rr^2}\dot{x}+\frac{m_{ch}.l}{(2m_{ch}+\frac{2J_w}{r^2}+m_{ch})}\ddot{\theta}+ \quad (12)$$
$$+\frac{Cu.n}{(2m_{ch}+\frac{2J_w}{r^2}+m_{ch})Rr}(V_{AL}+V_{AR})$$

By substituting equations 11 into equation 10 and equation 12 into equation 9 we are able to obtain state space equations of the system. Coefficients A_{22}, A_{23}, A_{42}, A_{43}, B_1 and B_2 are obtained from equations 11 and 12 [2].

$$\begin{bmatrix}\dot{x}\\ \ddot{x}\\ \dot{\theta}\\ \ddot{\theta}\end{bmatrix}=\begin{bmatrix}0&1&0&0\\0&A_{22}&A_{23}&0\\0&0&0&1\\0&A_{42}&A_{43}&0\end{bmatrix}\begin{bmatrix}x\\ \dot{x}\\ \theta\\ \dot{\theta}\end{bmatrix}+\begin{bmatrix}0\\B_2\\0\\B_4\end{bmatrix}\begin{bmatrix}V_{AL}&0&V_{AR}\end{bmatrix} \quad (13)$$

A. *Mathematical Model Simulations*

We simulate the dynamic model by applying the step of the control signal on the inputs of model. This excites oscillations of the chassis. Also disturbances affected on the chassis (applying torque on the chassis is affecting $\ddot{\theta}_{ch}$) excite oscillation. This disturbance is used in all simulations. This can be seen in Fig.5 and Fig.6. The mathematical model of the MAV is in stable position (at 180 deg.) in these simulations.

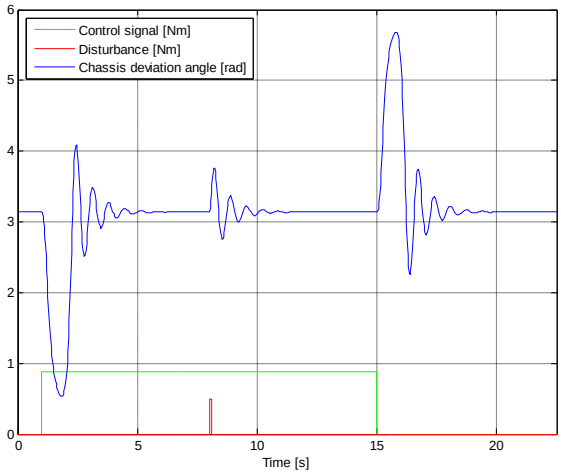

Figure 5. Oscillation of the chassis of the MAV

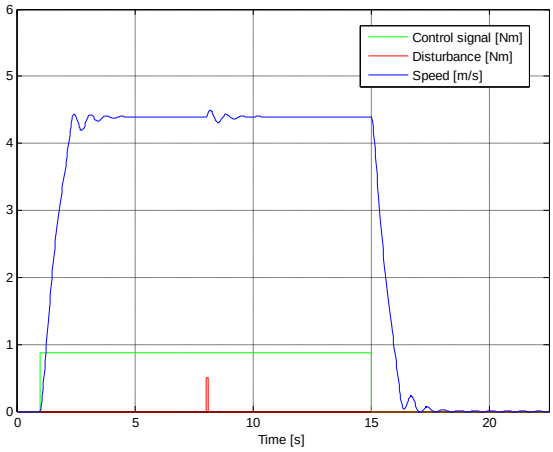

Figure 6. Oscillation of the speed of the MAV

III. OSCILLATION DAMPING

A. *Control Signal Shapers*

Changes of control signal (wheels speed is changing) are exciting oscillation (around lower position) in the MAV. This oscillation or this state of the MAV is called residual oscillation. To avoid this oscillation input signal shapers are usually used. As can be seen in Fig.7 the shaped signal is obtained by convolving desired input with the series of Dirac impulses.

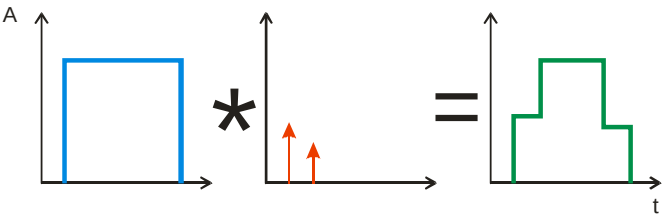

Figure 7. Basic principles of signal shaping methods

Basic type of shapers is Zero Vibration Shaper (ZV shaper). It uses only 2 impulses. The ZV shaper is sensitive to the changes of the system own natural frequency, therefore in our case we are using Zero Vibration Derivative Shaper (ZVD shaper). The ZVD shaper is less sensitive to changes of the system natural frequency and its uses 3 impulses. ZVD shaper for system with a natural damping *b* is de-scribed by following equation:

$$\begin{bmatrix} A_i \\ t_i \end{bmatrix} = \begin{bmatrix} \frac{1}{(1+k)^2} & \frac{2k}{(1+k)^2} & \frac{k^2}{(1+k)^2} \\ 0 & \frac{T_D}{2} & T_D \end{bmatrix}; k = e^{-\frac{b.\pi}{\sqrt{1-b^2}}} \quad (14)$$

where:

A_i Amplitude of i-th Dirac impulse

t_i Delay of i-th Dirac impulse

T_D Period of the system natural oscillation

Simulation scheme of the ZVD shaper is shown in Fig.8. [3].

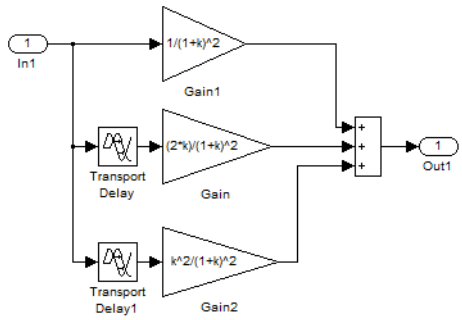

Figure 8. Simulation scheme of the ZVD Shaper

B. *Evaluation of the ZVD Shaper*

For evaluation we created a simulation model of damping control using ZVD shaper (Fig.9).

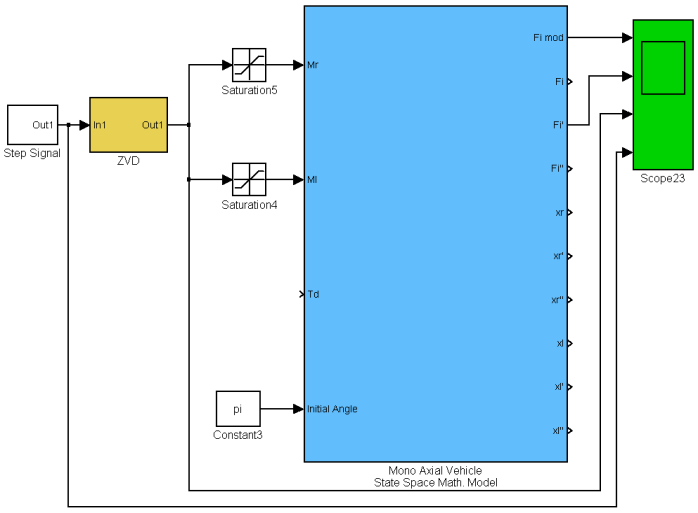

Figure 9. Simulation model of damping control using ZVD shaper

First we need to identify oscillation parameters of the MAV. Resonant frequency and period of the MAV was calculated as follows:

$$\omega_0 = \sqrt{\frac{m_{ch}.g.L}{J_{ch}}}; T_0 = \frac{2\pi}{\omega_0} \quad (15)$$

The damping ratio b was identified experimentally from the oscillation shown in Fig.5. ZVD shaper was set by using these parameters. The ZVD shaper was tested with the same input signal as was in the simulations above (Fig.5, Fig.6). Next two graphs (Fig.10, Fig.11) shows result of these simulations.

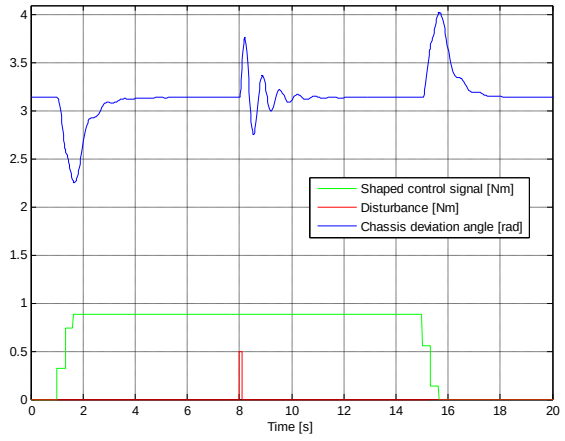

Figure 10. Graph of the chassis angle of the MAV when is used the ZVD shaper

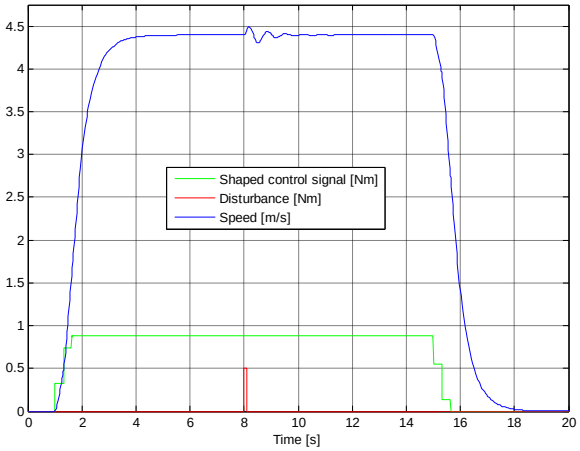

Figure 11. Graph of the velocity of the MAV when is used the ZVD shaper

C. *Derivative Feedback*

Next method is the derivative feedback. This method increases the naturally low damping ratio of systems to appropriate value. By using the derivative feedback we can move oscillating complex poles of the system into the position near to the real axis in the complex plane, so the damping ratio of the system will increase. Scheme of typical derivative feedback is illustrated in Fig.12. We want to damp oscillation of the chassis angle. We will use the signal of angular velocity of the chassis for feedback. So derivation of the angle output of model is not needed in this case, because it is available from the Mono Axial Vehicle simulation block. Derivative feedback gain was set experimentally. If the system contains yet another low damped pole pair, it can be destabilized easily. This might decrease effectiveness of this method.

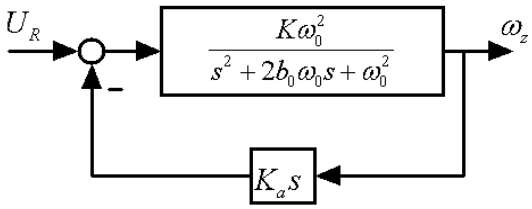

Figure 12. Typical structure of the control system with derivative feedback

From Fig. 12 we can define these parameters of system :

ω_0 natural frequency of a system

b_0 natural damping of a system

K system gain

K_a gain of the derivative feedback

We can calculate the gain of the derivative feedback by following equation:

$$K_a = \frac{2(b - b_0)}{K} \qquad (16)$$

where:

b desired value of system damping (optional)

D. *Derivative Feedback Evaluation*

As mentioned before we set derivative feedback experimentally. The value which gain feedback was finally set is equal to 0.23. Results of the simulations are visible in Fig.13 and Fig.14. Derivative feedback in comparison with the ZVD shaper is able to avoid even oscillation caused by the disturbances. Also by using this method the damping coefficient of the system was increased.

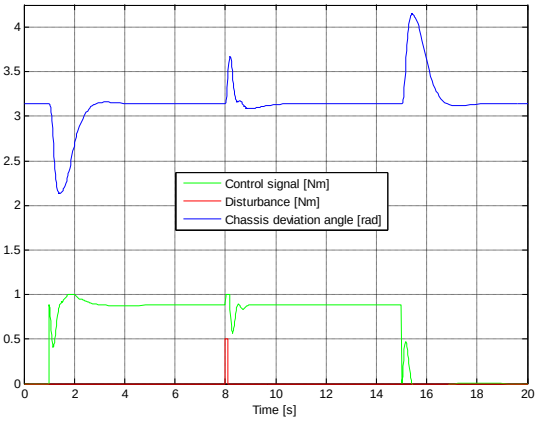

Figure 13. Graph of the chassis angle of the MAV when is used the derivative feedback

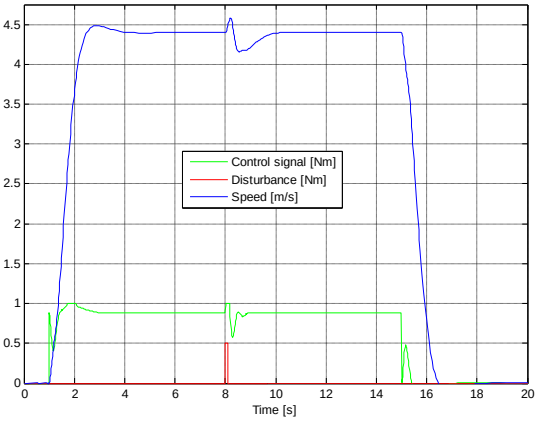

Figure 14. Graph of the velocity of the MAV when is used the derivative feedback

IV. THE LQR CONTROLLER FOR STABILIZING THE MAV

Linear Quadratic Regulator Controller is optimal state-feedback controller with good robustness for robotic applications (Fig.15). In fact the LQR controller is optimal pole placement controller.

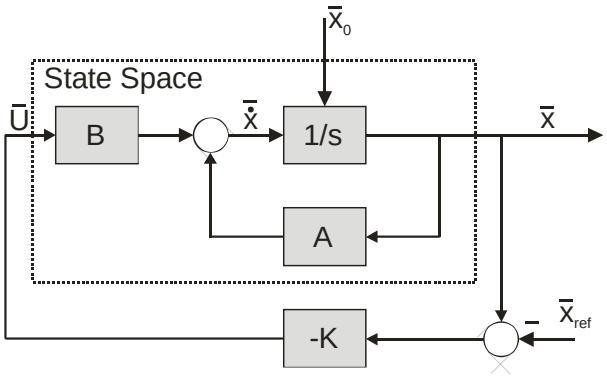

Figure 15. LQR controller

In order to design the LQR controller we need to get the linear state space model of the system as follows:

$$\dot{x} = Ax + Bu \qquad (17)$$
$$y = Cx$$

And the control law of LQR is defined by this equation:

$$u = -K(x - x_{ref}) \qquad (18)$$

The control gain K (19) is obtained from the infinite horizon performance index J (20) and the solutions of the Riccati equation for infinite horizon is (21).

$$K = R^{-1}B^T P \qquad (19)$$

$$J = \frac{1}{2}\int_{t_0}^{\infty}(x^T Qx + u^T Ru)dt \qquad (20)$$

$$0 = A^T P + PA - \dot{P}BR^{-1}B^T P + Q \qquad (21)$$

The matrices Q and R matrices are usually diagonal and first choice for these matrices can by given by using the Bryson's rule.

The LQR is a linear controller, therefore we have to linearise mathematical model of the MAV. Linearization of the dynamic model of the MAV can be done near an equilibrium of the MAV in upper position. In time of writing this paper we were still working on the LQR controller, therefore we didn't have any simulations available yet. [4]

V. Experimental Setup

Experimental MAV device is prepared for the efficiency measurement of proposed methods is based on the following hardware components:

Drive:

2 x MAXON RE35 90Watt (15.0V nominal voltage) + Planetary gearbox GP 42 C with ratio 12:1, IRC sensor HED–5540. Motor controller MAXON EPOS 24/5

Sensors:
3 axes accelerometer + 3 axes gyroscope, 2 axes magnetometer, laser scanner Hokuyo URG-04LX, Ultrasonic range sensors and GPS SiRFstar III receiver.

Accumulators:
4 – cells LiFePo A123 2200 mAh. Rated for 30C continuous discharge (66.6A)

Control board:
Based on dsPIC33FJ64GP306 (16 bit digital signal controller). This is used for low-level control (ZVD, LQG, Kalman Filtering etc.). Devkit 8000 based on OMAP3530 (ARM Cortex A8) for high-level control (navigation etc.).

Communication board:
Based on zigbee modules. This board will provide telemetry data and remote control for the MAV

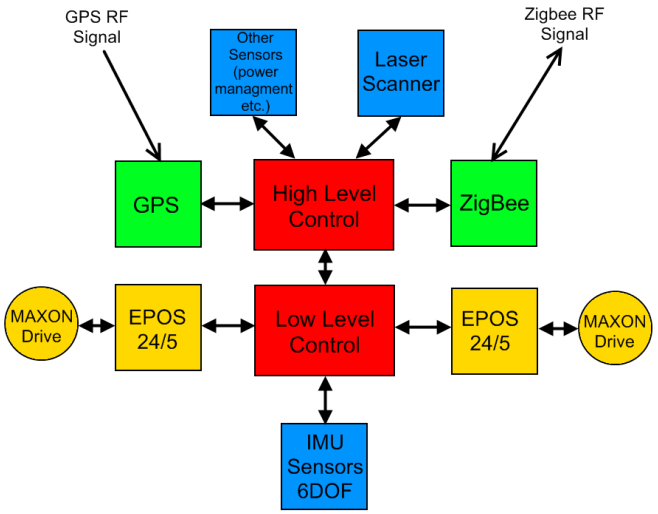

Figure 16. Block diagram of the MAV

Only part of the sensors is used for the damping of the oscillation and/or for stabilizing the platform, the rest is planned to be used for the navigation and obstacle avoidance or for other purposes followed from the application where the robot would is used. The block diagram of the experimental setup of the MAV is in Fig. 16. The second version of the MAV is being developed in these days. The Fig. 17 shows the part of the 3D virtual model of the MAV.

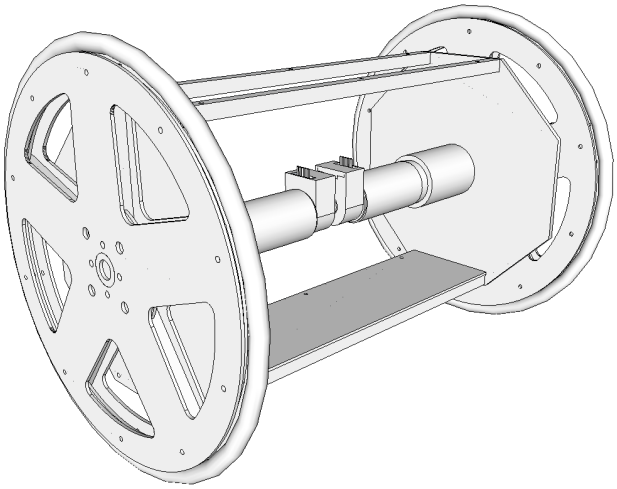

Figure 17. 3D virtual model of the MAV version 2

VI. CONCLUSION

This paper presents various control techniques to damp oscillation and optimal control of the MAV which can be used as platform for service mobile robots.

First we analyzed oscillation and designed ZVD shaper for damping oscillation. In next step we present derivation feedback, which is used for oscillation damping. ZVD shaper does not affect stability of the system, but it is also not able to damp oscillation caused by disturbances. The derivation feedback in comparison with the ZVD shaper is able to eliminate oscillation caused by disturbances, but it might destabilize the system. Next advantage of the ZVD shaper can be that it does not require any additional sensors. Also the ZVD shaper can be used if sensors fail. We can also combine these two methods for oscillation damping. For example we will use ZVD shaper during the phase of control signal change, but after this phase we will use derivation feedback.

We also showed basic principle of the LQR controller. Since we are still working on it during the time of writing this paper, the LQR control method is not described and evaluated here.

These control techniques describe just oscillation damping and stabilizing of the MAV. Next step will be to implement this hybrid control into real MAV and to implement methods for navigation in environment to the MAV [5]. Now we are also working on chassis of the MAV and on electronics for it. Chassis will be based on composites materials. The MAV will be driven by MAXON motors and planetary gear. Electronics is based on DSP microcontroller and MEMS sensors.

ACKNOWLEDGMENT

This work was supported by Grant Agency of Ministry of Education and Academy of Science of Slovak Republic VEGA under Grant No. 1/0690/09. The authors are pleased to the acknowledge this support.

[1] RODINA,J.-HUBINSKÝ,P.: Stability control design of segway like differential drive by using MEMS sensors, s.483-487, Metalurgija (Metallurgy) č.2, roč.49, 04-06/2010, Croatia, ISSN 0543-5846.

[2] GRASSER F., D'ARRIGO A., COLOMBI S., RUFER A.: JOE: A Mobile, Inverted Pendulum, Published in 2001 [online] http://leiwww.epfl.ch/publications/grasser_darrigo_colombi_rufer_mic_01.pdf

[3] SINGHOSE W., SINGER N., SEERING W.: Comparison of Command Shaping Methods for Reducing Residual Vibration, Published in 1995. [online] http://www.me.gatech.edu/inputshaping/Papers/ECC95.

[4] KOZÁKOVÁ A.: Design of discrete-time compensator for reference tracking with disturbance rejection. /Transactions of the VŠB - Technical University of Ostrava, Mechanical Series/, 2008, vol. LIV, No.2 (2008), 67-72. ISBN 978-80-248-1727-9

[5] BABINEC A., DUCHOŇ F.: Metódy reaktívnej navigácie mobilného robota v neznámom prostredí, Published in: Nové trendy v kybernetike, automatizácii a informatike : Odborný seminár. Gabčíkovo, Slovenská republika, 7.-9.9.2009. - Bratislava : STU v Bratislave FEI, 2009. - ISBN 978-80-227-3107-2. - CD-ROM